JOURNAL OF APPLIED ELECTROCHEMISTRY 26 (1996) 567–574

Electrochemical remediation of metal-bearing wastewaters
Part I: Copper removal from simulated mine drainage waters

T. L. HATFIELD, T. L. KLEVEN, D. T. PIERCE

Department of Chemistry, University of North Dakota, Grand Forks, ND 58202, USA

Received 12 July 1995; revised 10 November 1995

A bench-scale electrochemical cell for plating heavy metals, such as copper from dilute wastewaters, was designed and tested. Optimization tests were performed on simulated mine-drainage water (pH 2.6, 0.1 M Na_2SO_4, 0.02 $\Omega^{-1}cm^{-1}$, 150 mg L^{-1} Cu^{2+}) using a vertically oriented, flow-through cell containing a carbon felt cathode. Results obtained for optimized conditions of applied potential and volume flow rate demonstrated greater than 99.9% recovery of copper metal from feed solutions at an ohmic corrected potential of −0.70 V vs Ag/AgCl and flow rates approaching the design maximum of about 0.30 mL s^{-1}. The effluent concentration of copper under conditions of optimum potential and flow rate could be routinely reduced to a target level of 50 $\mu g\,L^{-1}$.

1. Introduction

The direct discharge of metal-contaminated drainage and run-off from mining sites poses a serious environmental threat that has intensified in mineral-rich districts throughout the United States [1]. Federally regulated concentrations for discharge of heavy-metals such as copper, lead, cadmium and mercury into the environment have steadily declined since the passage of the 1972 Clean Water Act (CWA) and the 1974 Safe Drinking Water Act (SDWA) [2]. Particularly, amendments to the SDWA and CWA in 1986 specified 13 metals, including the four listed above, as priority pollutants and established maximum discharge levels for most of these metals in the sub-ppm (mg L^{-1}) to low ppb ($\mu g\,L^{-1}$) range [3]. At these present safe-release levels, the costs for remediation of mineralized wastewaters pose a sizable and growing burden to nearly all metals processing industries [4].

Traditionally, the large-scale treatment of metal-bearing waters has been carried out by sludge precipitation and landfill methods [5]. These procedures, however, are clearly not a final solution to metal-contamination problems because they merely shift the heaviest treatment responsibilities from tasks of metal removed to the increasingly difficult tasks of solid waste transportation and stabilization. Regulatory approval as well as the continuous liability associated with even carefully researched landfills are now major drawbacks to these traditional forms of water treatment. One strategy for long-term and economical clean-up of mineralized wastewaters is to consider dissolved and hazardous metals as a resource to be quantitatively recovered and potentially marketed. This simultaneous concern for remediation and capture of mineral assets can only be successful if contaminants can be selectively and quantitatively removed.

Electrochemical forms of remediation satisfy these requirements and offer terminal processes for recovering metal contaminants at sites in need of continuous wastewater treatment [5–11]. However, despite electrochemical systems being used and marketed for many years to recover metals from concentrated mining liquors, as well as from industrial photofinishing and electroplating solutions [8, 9, 11], far fewer methods have been devised for the remediation of relatively dilute wastewaters such as those generated from mine drainage or run-off [5, 8].

The work described herein was directed towards the construction and testing of a prototype electrochemical cell that efficiently plates and thereby eliminates metal contaminants from dilute waste streams. The cell uses a single-pass, flow-through design that channels wastewater through a porous plating electrode. This configuration allows large volumes of dilute waters to be economically treated and is one of the more standard configurations used for large-scale electrochemical processing [12]. A notable feature of the present cell design is the use of a carbon felt as the electrode material. Carbon remains the electrode material of choice for most electrodeposition applications because it is conductive (with a high overpotential for proton reduction), it is light, and it is relatively inexpensive. Microfibrous carbon felts have also been the focus of many mass transfer studies involving electrodeposition reactions and have been shown to achieve high plating efficiencies for a variety of metals [13–17]. Despite

0021-891X

this large amount of related work, the use of carbon felt for tasks of continuous water remediation continues to remain poorly documented [18, 19].

Design criteria and the results from optimization experiments are reported herein for the bench-scale extraction of copper from simulated mine drainage waters using a carbon felt, flow-through cell. Extraction of copper from actual mine drainage waters with this same cell design and the effects of side reactions from interfering components will be addressed in a forthcoming paper [20].

2. Experimental details

2.1. *Materials, instrumentation, and procedures*

All solutions were prepared with 18 MΩ cm Milli-Q reagent water (Millipore Corp.). Unbuffered, aqueous electrolyte solutions were employed in all electrochemical experiments. All were prepared with Na_2SO_4 (reagent, EM Science) and concentrated H_2SO_4 (technical, MCB). Precise pH measurements were performed with a glass membrane electrode (Sigma, E-4503) and Corning model 12 meter. Copper sulfate (reagent, Mallinckrodt) was dissolved in stock electrolyte to produce mineralized solutions of known concentration (±0.1%) that were used to test the performance of the electrodeposition cell, as well as to calibrate copper response detected by flame atomic absorption spectroscopy (FAAS) and anodic stripping voltammetry (ASV). No precautions were taken to deoxygenate solutions prior to testing.

Copper concentrations in all electrochemically treated solutions were initially screened by FAAS with a Perkin–Elmer spectrometer (model 2280) aligned to the 324.75 nm hollow-cathode emission of copper. Only when concentrations were found to be below the 10 mg L^{-1} detection limit of the FAAS instrument were they measured by ASV with a 303 hanging mercury drop electrode (EG&G, PARC model) and potentiostat (PAR model 174). FAAS and ASV analysis' were accurate to within ±1%.

2.2. *Cell design and operation*

The bench-scale cell that was tested was similar to the device of Wenger and Bennion [21], with the exception of the electrode material. The cell body, shown in Fig. 1, was fabricated from clear acrylic and contained cylindrical (inner diameter = 5.1 cm, lengths = 1.9, 4.4, or 7.0 cm), flow-through electrode compartments at each end of a central quieting chamber.

Cathode and anode compartments were loaded with about 1.5 to 4.5 g of carbon felt (Amoco Thornel Mat VMA, 1.4 Ω^{-1} cm^{-1}, 0.4 m^2 g^{-1}, fibre diameter 13 μm, porosity 0.98) and perforated stainless steel plates provided electrical contact at the exits of both electrodes. The anode compartment entrance was covered with 40 × 40 mesh copper screen to provide a low voltage counter reaction and to prevent

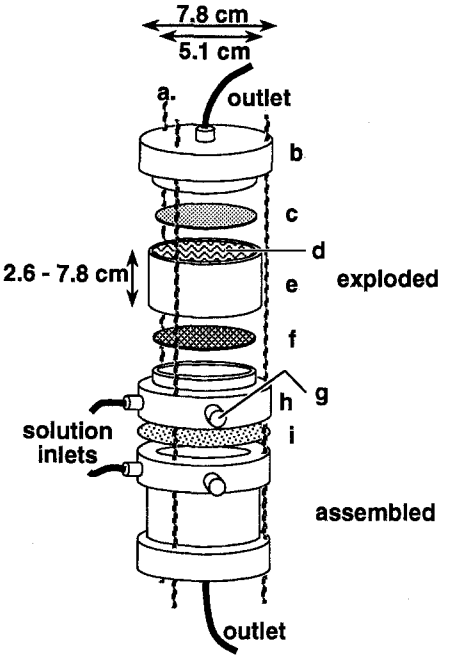

Fig. 1. Nonscale drawing of copper electrodeposition cell, showing assembled (bottom) and disassembled (top) electrode compartments. Parts designated are 1/8 in dia. threaded rod (a), electrode end-cap (b), perforated stainless steel electrode-contact (c), carbon felt electrode material (d), electrode compartment (e), plastic or copper 40 × 40 mesh inlet screen (f), reference electrode fitting (g), electrode inlet/solution quieting chamber (h), and optional cellulose acetate membrane (i). Neoprene o-rings and gaskets have been omitted for clarity.

oxygen evolution. The cell was assembled under water to ensure proper wetting of the carbon felt and to eliminate air pockets which caused channelling of solution within the electrode compartments. It was found that loading the carbon felt with the majority of the fibres parallel to the flow axis of the compartments allowed any residual gas bubbles to move easily through an electrode. Standardized test solutions were suspended 1.5 m above the assembled cell (Fig. 2) to provide sufficient head pressure for flow rates up to 20 mL s^{-1}.

Solutions passed through a main valve into the central quieting chamber and subsequently into

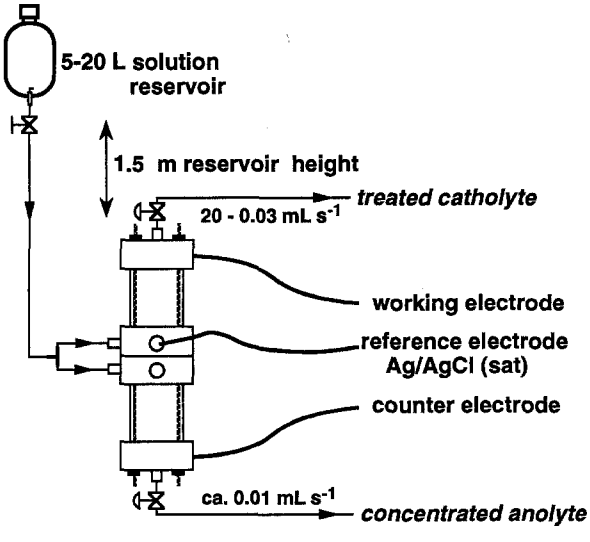

Fig. 2. Schematic diagram of the fully assembled cell, solution inlets/outlets, valves, electrode leads and solution reservoir.

the opposing cathode and anode compartments of the cell. Metering valves positioned at each electrode exit independently controlled solution flow through these compartments. Flow rates were measured to a precision ±5% by timing the collection of measured volumes of the cell effluent. No precaution was made to thermostat the cell during operation. However, all experiments were performed at ambient temperatures of 24 ± 3 °C.

An EG&G PARC 273 potentiostat was used to control cathode voltage relative to a fritted Ag/AgCl (saturated) reference electrode positioned at the entrance of the cathode compartment (labeled 'g' in Fig. 1). Cell currents as well as catholyte copper concentrations and pH were only recorded after the cell current reached a steady-state value. This condition usually required the elution of 300–500 mL of catholyte, after which the current usually remained within ±0.1 mA.

3. Results and discussion

3.1. *Electrochemical system*

Table 1 gives a partial assay of drainage water collected from the 6 m level of the closed Berkeley copper mine pit in Butte, Montana. This listing of major components illustrates the diversity of metal ions found at many open pit mining sites throughout the middle United States [22]. It also points out the advantage that might be gained if only harmful components could be selectively and economically extracted from the bulk liquid.

Table 1. Screening of major elements in real and simulated samples of mine drainage waters

Parameter	*Actual mine water**	*Simulated mine water†*
Elements ($mg\,L^{-1}$)		
Al	120	
Ca	440	
Cd	2.0	
Co	0.9	
Cu	180	150
Fe	320	
K	9.3	
Mg	440	
Mn	210	
Na	74	4600
Si	46	
Zn	510	
Anions ($mg\,L^{-1}$)		
Cl^-	16	
SO_4^{2-}	6900	9600
Conductivity ($10^3\,\Omega^{-1}\,cm^{-1}$)	4.21	18.6
pH	2.87	2.80

* Sample recovered from 2 m level of Berkeley Mine Pit (Butte, MT, USA). Elemental analysis' were performed by inductively coupled argon plasma and anion analysis' were performed by conventional ion chromatography.

† Sample used for testing electroremediation cell. Elemental and anion concentrations were based on component weights used to prepare test solution.

A matrix with this degree of complexity demands that performance of any extraction cell first be tested and then optimized with a simplified electrochemical system that targets the species of greatest interest and concentration. The test solution selected for cell characterization in this work (col. 2, Table 1) approximated the copper content, pH, conductivity and anion composition of actual drainage water samples extracted from the Berkeley mine pit. Effects of other major components, such as iron, were addressed in subsequent work explicitly aimed at electrochemically treating the Berkeley pit water [20].

At the cathode, the principle reaction that occurred with the test solution at moderate negative potentials was the deposition of copper. Although this reaction competed at more negative potentials with the reduction of proton, bubble nucleation from the production of hydrogen could usually be avoided. At the anode, oxidation of water to produce oxygen was avoided by facing the anode compartment with copper mesh screen or by inverting the cell to make the copper plated cathode the anode. Here, the dissolution of copper not only provided a low-voltage counter reaction, it also produced a highly concentrated stream of copper ions (usually >0.1 M) when the anolyte flow rate was slowed significantly below the flow rate of the catholyte. At this concentration level, copper from the anolyte solution could be easily recovered by conventional hydrometallurgical methods [23]. This utilization of the entire electrochemical system for the purpose of selective extraction, concentration, and recovery was first developed by Bennion and Newman [21] but has since received little attention.

3.2. *Effects of cell orientation and membrane separator*

The crucial nature of cell orientation was evident during initial testing of the cell. Early trials demonstrated plating yields (R in Equation 1) of less than 30% when the flow-axis of the cell was held horizontally or held vertically with the anode on top.

$$R = 1 - (C_{out}/C_{in}) \qquad (1)$$

where C_{in} and C_{out} were the concentrations of copper entering and exiting the cathode, respectively. These results persisted regardless of applied voltage and were only marginally improved when a cellulose acetate membrane divided the quieting chambers ('i' in Fig. 1) or when longer cathodes were employed (e.g., 4.4 or 7.0 cm). The poor yields were traced to gravitational flow of concentrated (and therefore more dense) anolyte copper into the cathode compartment. When the cell was operated horizontally, a blue flow of concentrated cuprous ions could be viewed as it passed out of the anode compartment, along the bottom of the transparent quieting chamber, and into the cathode compartment. Dissection of the cathode felt after such a trial showed that copper was deposited through the entire length

of the carbon plug and only along a thin band that had been at the bottom of the compartment.

By operating the cell vertically, with the anode at the bottom, the gravitational flow of concentrated anolyte copper was directed away from the cathode compartment. In this orientation, significant removal of catholyte copper ($R > 95\%$) was consistently achieved under mass-transfer limited conditions and no membrane was required to separate the opposing electrode compartments. Moreover, greater than 99.99% removal was obtained with the shortest electrode length tested (1.9 cm), indicating that the catholyte could be depleted of copper even within a relatively short distance after entering the electrode. Accordingly, all polarization tests were conducted with the cell axis held vertically, with the cathode as the uppermost electrode compartment, and without an interelectrode membrane.

3.3. *Behaviour of cell under polarization*

Figure 3 shows steady-state polarization curves exhibited by the cell for the standardized test solution described in Table 1. At the lowest flow rates, the cell consistently demonstrated a region of little or no current change (Fig. 3(a)) that was indicative of a mass-transport limited reaction throughout the cathode. Because these plateaus were only observed at potentials where significant copper deposition occurred, as evidenced by large decreases in cupric ion concentration in the catholyte effluent (Fig. 3(b)), the reaction was certainly one involving copper deposition. This latter fact was further supported by the good correlation between measured plateau currents and limiting currents predicted by Equation 2 for quantitative copper removal ($R \simeq 1.0$) with 100% current efficiency (horizontal lines in Fig. 3(a)),

$$I_{\text{lim}}(Cu^{2+}/Cu^{0}) = 2FURC_{\text{in}} \qquad (2)$$

where F is the Faraday and U is the volume flow rate.

An important observation from the standpoint of remediation was that the catholyte consistently demonstrated cupric ion concentrations in the sub-ppm range when the cell was operated at potentials and flow rates where the plating reaction was transport limited throughout the cathode (i.e., where current plateaus were observed). Under this condition, the effluent cupric ion concentration could be effectively decreased by a factor of 10^4 or more and the electrodeposition process was clearly viable with chemical or other methods of metal removal [5].

A second polarization effect apparent from Fig. 3(a) was an increase in current at potentials negative of each observable transport-limited plateau. Because Equation 2 accurately predicted the magnitude of mass-transfer limited current for the copper plating reaction (assuming a 100% current efficiency), the higher than expected currents were the result of a second electrode reaction. The most likely candidate, proton reduction, was confirmed by pH measurements

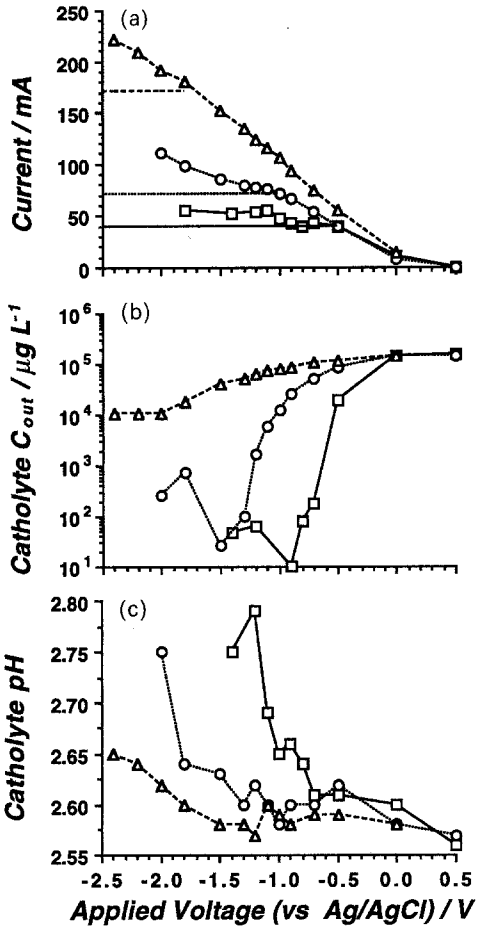

Fig. 3. Polarization curves showing (a) steady state current (in mA), (b) copper ion concentration in the catholyte effluent (in $\mu g\,L^{-1}$), and (c) catholyte effluent pH at flow rates of 0.083 (solid line + squares), 0.15 (dotted line + circles), and 0.38 (dashed line + triangles) $mL\,s^{-1}$. Limiting currents (horizontal lines) in (a) calculated from Equation 2 for each flow rate. Cathode length and mass of carbon felt were 1.9 cm and 1.7 g, respectively. Entering solution composition was 150 $mg\,L^{-1}$ Cu^{2+} and 0.10 M Na_2SO_4 (pH 2.60 ±0.03).

of the catholyte effluent (Fig. 3(c)). At potentials positive of the current plateau, the catholyte pH was not significantly altered after passage through the cell and remained near its original value of 2.60 ± 0.03. However, at more negative potentials the pH increased measurably, indicating that proton was consumed by reduction at the cathode. It was observed that once the catholyte pH exceeded a value of 2.70, generation of hydrogen was sufficiently rapid to observe bubble nucleation at the cathode entrance. It was also observed that the catholyte pH measured at a particular applied voltage and flow rate had a small but discernible dependence on the amount of copper deposited. Specifically, the rate of proton reduction appeared to increase after a significant amount of dendritic copper had been deposited onto the felt cathode. Rate enhancements for proton reduction at electrodeposited copper have been reported for other carbon-based flow-through cells [17].

A third characteristic evident from Fig. 3(a) was an apparent shift of the plateau current to more negative potentials as flow rate was increased. This feature was the result of electrolyte resistance that coupled

ohmicly with any current passing at the surface of the cathode. Coupling of this nature generally leads to voltage errors or drops that are directly proportional to the cathode current as well as the solution resistance through which the current passes. Two distinct cell regions expressed ohmic coupling and these sources combined to give the negative shift seen in Fig. 3(a).

The region with the largest ohmic coupling was the thin layer of solution between the cathode entrance and the upstream reference electrode ('g' and 'f' in Fig. 1, respectively). In this region, the voltage drop was dictated by the total cathode current and was decreased with smaller reference/cathode distances. Although the coupled resistance was minimized by positioning the reference electrode as close as possible to the cathode entrance face (~ 2 cm), an estimated 6.8 Ω solution resistance still remained. Determination of this value is described in Appendix 1. Multiplying this resistance with steady state currents in Fig. 3(a) gave voltage drop errors at each point on the polarization curves. These errors were then removed by difference from the potential axis. The corrected family of curves shown in Fig. 4(a)–(c) demonstrated no shift for proton reduction onset (vertical lines at −0.70 V vs Ag/AgCl) as expected for upstream placement of auxiliary and reference electrodes [23, 24].

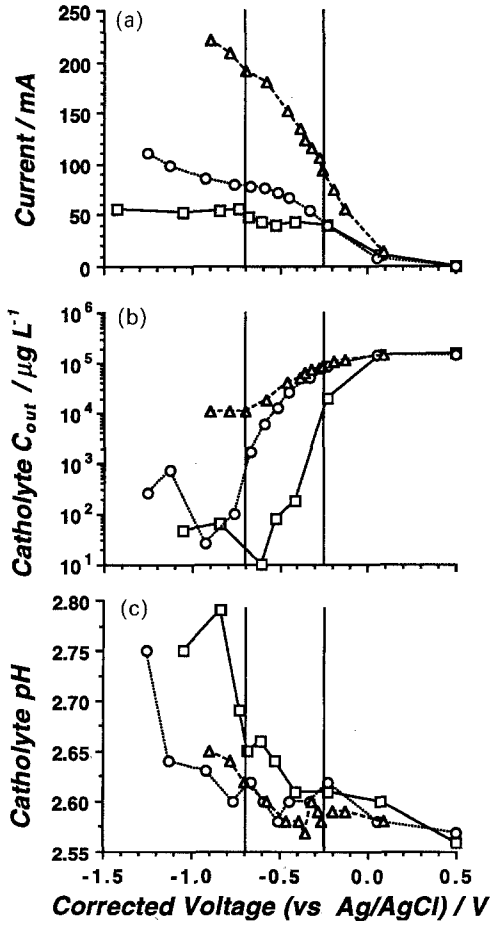

Fig. 4. Polarization data from Fig. 3 plotted with 6.8 Ω corrected potential axis for all curves. Lines at −0.70 V vs Ag/AgCl correspond to the onset of proton reduction reaction. Lines at −0.25 V vs Ag/AgCl correspond to the onset of mass-transfer controlled deposition of copper at 0.083 mL s^{-1}.

However, the potential at which a current plateau was reached (Fig. 4(a)), or at which a significant amount of copper was removed (Fig. 4(b)), still appeared to shift to more negative voltages as flow rate was increased.

This apparent shift of plateau current and effluent composition, even after correcting for ohmic coupling near the upstream reference electrode, was the result of voltage drops within the cathode itself. Assuming a plug-flow model and negligible potential variation along the cathode matrix, Bennion and Newman first described the solution potential drop through the length of a porous, flow-through cathode and showed that the drop occurs in direct proportion to the current that passes at each cathode cross-section [21]. For the specific application of copper removal, the solution voltage drop through the cathode caused the overpotential for copper deposition to decrease continuously at more downstream segments. Results of this effect can be easily seen in Fig. 4(a) at the corrected potential of −0.25 V vs Ag/AgCl (rightmost vertical line). Only at the lowest flow rate was the voltage drop sufficiently small that the plateau current was obtained, indicating that copper deposition was mass-transfer controlled *throughout* the cathode. At higher flow rates, the voltage drop through the cathode was more severe because proportionally greater currents were generated at each cathode segment. In these cases, net currents were far below than their plateau limits indicating that mass-transfer control was lost before the catholyte could exit the cell. Because mass-transfer control could only be regained by applying greater overpotentials relative to the upstream reference electrode, the net result of ohmic coupling within the cathode was to shift the copper deposition *plateau* to more negative potentials at higher flow rates. Quantification of this effect, as outlined in the following section, was needed to predict the optimal flow rate for copper removal.

3.4. *Optimum operating parameters*

Optimization of copper removal with the cell in Fig. 1 primarily hinged on the condition of quantitative removal of copper ion from the feed solution. To meet this criterion, the copper deposition process had to proceed under mass-transfer control throughout the cathode. Other requirements were that the deposition reaction proceed without any interference from side reactions, such as the reduction of proton, and that the catholyte volume be processed as rapidly as possible. To ensure that each of these design criteria were simultaneously maintained, an optimum operating voltage and a maximum catholyte flow rate were the first parameters defined.

It was clear from the assessment of ohmic coupling in the cell that an optimum operating voltage for copper deposition should be as far negative as possible to avoid the loss of mass-transfer control at high flow rates. However, the most negative operating voltage for 100% efficient copper removal from the test

solution was limited by the onset of proton reduction. Because this reaction first occurred at the cathode entrance face where potential was controlled versus the reference electrode, the optimum potential was easily identified after correction for ohmic coupling within the reference/cathode gap. Inspection of the corrected curves in Fig. 4(a) and (c) showed that the most negative voltage reached before the detection of proton reduction was about −0.70 V vs Ag/AgCl (vertical lines) for all flow rates. Therefore, this potential corresponded to the optimal deposition voltage for copper ion.

To determine the maximum catholyte velocity, u_{max}, it was necessary to account for ohmic drop through the cathode under conditions of quantitative extraction. Bennion and Newman derived an order of magnitude approximation in Equation 3 that estimates u_{max} when the solution conductivity (κ), maximum cathode potential drop ($|\Delta\Phi|_{max}$), specific electrode area (a), and the mass-transfer coefficient (k_m) of copper ion are known [21].

$$|\Delta\Phi|_{max}\left(\frac{Cu^{2+}}{Cu^{0}}\right) = 2FC_{in}u_{max} \times \frac{1}{\kappa} \times \frac{u_{max}}{ak_m} \quad (3)$$

Using the maximum drop of 0.2 V suggested by Bennion and Newman for the removal of copper ion from solution [21], the specific active area of $2.4 \times 10^2\,cm^{-1}$ measured by Vatistas *et al.* for carbon felt of the type used in this work [16], and the mass-transfer equation empirically derived by Carta *et al.* for reactions at carbon felts in flowing streams [17], a maximum volume flow rate of $0.30\,mL\,s^{-1}$ was calculated for the copper test solution. Details of this calculation are given in Appendix 2.

The final design parameter to be determined was the minimum cathode length (L_{min}) needed to achieve a target effluent concentration. Using the concentration profile predicted for the flow axis of the porous cathode under conditions of mass-transfer control, Equation 4 [25],

$$\frac{C_{out}}{C_{in}} = \exp\left(\frac{-ak_mL_{min}}{u_{max}}\right) \quad (4)$$

and substituting the specific cathode area of $2.4 \times 10^2\,cm^{-1}$ [16] and the mass transfer expression of Carta *et al.* [17] as for Equation 3, a L_{min} of 4.4 cm was determined for a target catholyte concentration of $50\,\mu g\,L^{-1}$ from a feed stream containing $150\,mg\,L^{-1}$ copper ion.

The optimization method as well as calculated optimum operating parameters were confirmed by polarization tests shown in Fig. 5.

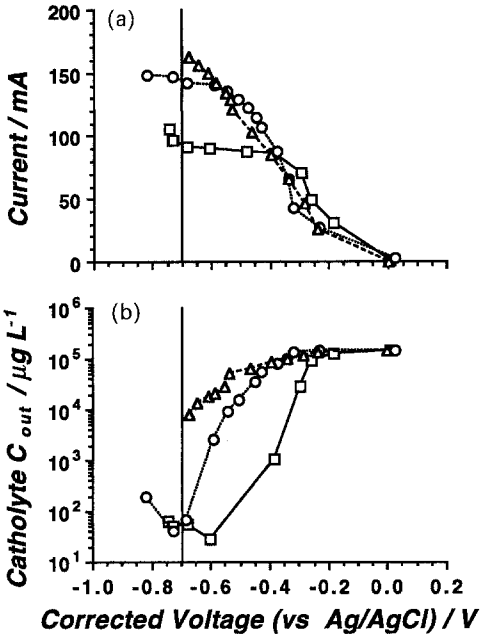

Fig. 5. Ohmic corrected (10 Ω) polarization curves showing (a) steady state current (in mA) and (b) copper ion concentration in the catholyte effluent (in $\mu g\,L^{-1}$) at flow rates of 0.15 (solid line + squares), 0.27 (dotted line + circles) and 0.30 (dashed line + triangles) $mL\,s^{-1}$. Lines at −0.70 V vs Ag/AgCl correspond to the onset of proton reduction reaction. Cathode length and mass of carbon felt were 4.4 cm and 3.8 g, respectively. Entering solution composition was $150\,mg\,L^{-1}$ Cu^{2+} and 0.10 M Na_2SO_4 (pH 2.60 ± 0.03).

Table 2. Compiled design parameters and optimal operating conditions for copper removal from simulated mine drainage water

Parameters	*Symbol*	*Value*	*Ref.*
Design			
Diffusion coefficient (Cu^{2+})	D	$7.5 \times 10^{-6}\,cm^2\,s^{-1}$	[17]
Kinematic viscosity (Cu^{2+}, SO_4^{2-})	ν	$1.024 \times 10^{-4}\,cm^2\,s^{-1}$	[17]
Feed concentration, copper	C_{in}	$150\,mg\,L^{-1}$	*
Effluent concentration, copper	C_{out}	$50\,\mu g\,L^{-1}$	*
Bulk solution conductivity	κ^0	$0.0186\,\Omega^{-1}\,cm^{-1}$	*
Conductivity within cathode pores	κ	$0.0178\,\Omega^{-1}\,cm^{-1}$	†
Cathode porosity	Θ	0.98	‡
Cathode cross-sectional area	A	$20.43\,cm^2$	*
Specific area of cathode	a	$2.4 \times 10^2\,cm^{-1}$	[16]
Optimized			
Maximum volume flow rate	U_{max}	$0.30\,mL\,s^{-1}$	*
Minimum cathode length	L_{min}	4.4 cm	*
Optimum corrected potential	E_{opt}	−0.70 V vs Ag/AgCl	*

* Based on this work.
† Calculated from $\kappa = \kappa^0\,(2\Theta/(3-\Theta))$ [17].
‡ Based on manufactured porosity and cathode loading density.

With the optimum cathode length of 4.4 cm, the ohmic corrected polarization data in Fig. 6(a) showed the same onset potential for proton reduction (−0.70 V vs Ag/AgCl, vertical line) as determined in previous experiments (Fig. 4). At flow rates approaching the design maximum of 0.30 mL s^{-1}, the mass-transfer limited current for copper deposition was shifted negatively and was truncated by the proton reduction threshold. The polarization curves measured at a flow rate of 0.27 mL s^{-1} were the most significant. These curves showed the last evidence of a current plateau (Fig. 5(a)) as well as a 50 μg L^{-1} concentration of copper in the catholyte effluent (Fig. 5(b)) at the optimum deposition voltage of −0.70 V vs Ag/AgCl. Curves at only marginally higher flow rates, such as 0.30 mL s^{-1} in Fig. 5, showed no current plateau and the effluent copper concentrations were consistently greater than 1 mg L^{-1}.

4. Conclusions

Table 2 summarizes the optimum design and operating parameters that were determined for copper removal with the flow-through, carbon felt cell presented in this work.

Applied to the acidic waste stream that was moderately conductive (0.02 Ω^{-1} cm^{-1}) and contained a moderate mineral loading (150 mg L^{-1} Cu^{2+}), the benchscale cell demonstrated greater than 99.9% recovery of copper metal from feed solutions at flow rates approaching the designed maximum of 0.30 mL s^{-1}. Although vertical orientation of the flow axis was necessary for high copper recovery, a membrane separating the anode and cathode compartments was not needed for efficient operation. Significantly, the typical effluent concentrations of copper measured at the design optimum potential and flow rate were routinely below the environmental discharge level of 1.3 mg L^{-1} [3] and generally below the design minimum of 50 μg L^{-1}. Extraction of copper from actual mine drainage waters using this same cell design will be described in a forthcoming article [20].

Acknowledgements

We thank D. Hassett, J. Thompson, F. Beaver and J. Harju of the UND Energy and Environmental Research Center for permission to quote unpublished results from their detailed analysis drainage waters from the Berkeley Pit Site. We also acknowledge the generous support the US Bureau of Mines under allotment grant G1134238 for TLH and North Dakota EPSCoR for the grant of a National Science Foundation REU assistantship to TLK.

References

[1] C. A. Hodges, *Science* **268** (1995) 1305.
[2] D. T. Reed, I. R. Tasker, J. C. Cunnane and G. F. Vandegrift, *in* Environmental Remediation. Removing Organic and Metal Ion Pollutants', *ACS Symposium Series 509* (edited by G. F. Vandegrift, D. T. Reed and I. R. Tasker), American Chemical Society, Washington (1992) p. 1.
[3] 40 CFR (Code of Federal Regulations) 264.94, Table I.
[4] P. H. Abelson, *Science* **255** (1992) 901.
[5] W. J. Eilbeck and G. Mattock, 'Chemical Processes in Waste Water Treatment', John Wiley & Sons, New York (1986).
[6] L. E. Vaaler, *AIChE Symp. Ser.* **77** (1981) 171.
[7] V. A. Ettel, *ibid.* **77** (1981) 183.
[8] J. L. Weininger, *ibid.* **79** (1983) 179.
[9] J. Farka and G. D. Mitchell, *ibid.* **81** (1985) 57.
[10] E. Avici, *J. Appl. Electrochem.* **18** (1988) 228.
[11] D. Pletcher, F. C. Walsh and I. Whyte, *Inst. Chem. Eng. Symp. Ser.* **116** (1990) 195.
[12] R. E. Sioda and K. B. Keating, *Electroanal. Chem.* **12** (1982) 1.
[13] K. Kinoshita and S. C. Leach, *J. Electrochem. Soc.* **129** (1982) 1993.
[14] Y. Oren and A. Soffer, *Electrochim. Acta* **28** (1983) 1649.
[15] B. Delonghe, S. Tellier and M. Astruc, *ibid.* **35** (1990) 1368.
[16] N. Vatistas, P. F. Marconi and P. F. Bertolozzi, *ibid.* **36** (1991) 339.
[17] R. Carta, S. Palmas, A. M. Polcaro and G. Tola, *J. Appl. Electrochem.* **21** (1991) 793.
[18] C. Zur and M. Ariel, *ibid.* **11** (1981) 639.
[19] *Idem, ibid.* **12** (1982) 231.
[20] T. L. Hatfield and D. T. Pierce, unpublished results.
[21] D. N. Bennion and J. Newman, *J. Appl. Electrochem.* **2** (1972) 113.
[22] 'Minerals Yearbook', Vol. I, *Metals and Minerals*, United States Department of the Interior, Bureau of Mines, Washington DC (1992).
[23] J. A. Trainham and J. Newman, *J. Electrochem. Soc.* **124** (1977) 1528.
[24] *Idem, ibid.* **125** (1978) 58.
[25] R. S. Wenger and D. N. Bennion, *J. Appl. Electrochem.* **6** (1976) 385.
[26] J. S. Newman, 'Electrochemical Systems', 2nd. ed., Prentice Hall, Englewood Cliffs, NJ (1991) pp. 487–91.

Appendix 1: Ohmic drop calculation

Ohmic drop between the upstream reference electrode and cathode entrance (R_{ohm}) in the designed cell was estimated from the potential shift of proton reduction onset, since this reaction occurs first at the cathode entrance where the overpotential is greatest. The potential for proton reduction onset, E_H, was extracted from each of the smoothed curves of Fig. 3(c) as they passed through the pH threshold of 2.63. Differences between these values as well as corresponding steady state currents, I_H, were then substituted into the Ohm's law relationship of Equation 5 to estimate an average value for R_{ohm}.

$$|\Delta I_H| R_{ohm} = |\Delta E_H| \quad (5)$$

Appendix 2: Maximum flow rate calculation

To solve for u_{max} in Equation 3, a relationship was required for the mass-transfer term, ak_m. The comprehensive study of laminar flow mass-transfer to flow-through electrodes by Cata *et al.* showed that the dimensionless mass-transfer expression in Equation 6 holds for a wide variety of carbon felts and other porous electrode materials [17].

$$Sh = 3.19 \times Re^{0.69} \quad (6)$$

Assignment of dimensioned parameters defined in Table 2 for dimensionless Sherwood (Sh) and

Reynolds (Re) numbers yielded an expression for ak_m that was substituted into Equation 3. The final expression for maximum catholyte velocity (Equation 7) is applicable to any carbon felt flow-through extraction cell operating under total consumption conditions.

$$u_{max} = \left[|\Delta\Phi|_{max} \times \frac{\kappa}{2FC_{in}} \times \frac{0.313\,D}{4\theta} \times \left(\frac{4\theta}{\nu}\right)^{0.69} \right]^{0.76} a \tag{7}$$

It is notable that the form of this hybrid expression clearly agrees with Newman's predictions that $|\Delta\Phi|_{max}$ should be proportional to $(u_{max})^{1.5}$ and to $a^{-1.5}$ for any flow-through reactor [26].